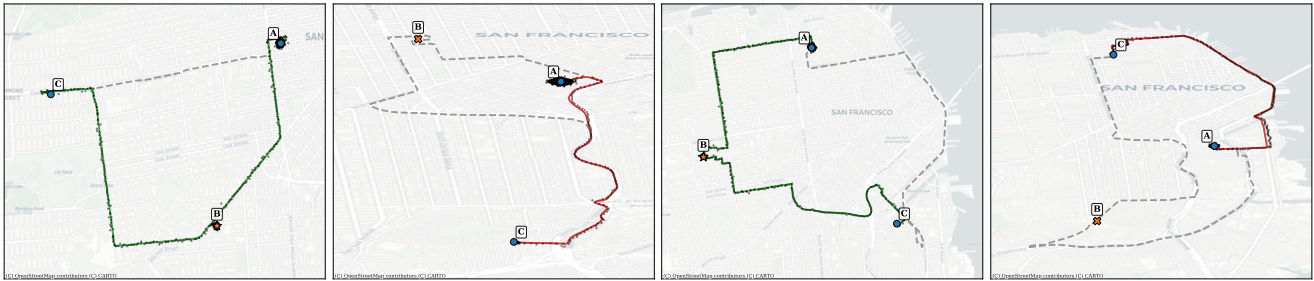


# Mobility Anomaly Generation using LLM-Driven Behavior with Kinematic Constraints (Systems Paper)

Yueyang Liu  
Emory University, Atlanta, USA  
yueyang.liu@emory.edu

Joon-Seok Kim  
Emory University, Atlanta, USA  
joonseok.kim@emory.edu

Andreas Züfle  
Emory University, Atlanta, USA  
azufle@emory.edu



**Figure 1: Examples synthetic trajectory modification: Insertion of new trips to a new Location B in-between two Locations A & C (1st and 3rd subfigure) and removal of visited Location B creating a direct trajectory between Locations A & C (2nd and 4th subfigure). Dashed grey lines denote the original trajectory. Solid green and red lines denote trajectories generated as described in this work. Black dots along trajectories denote generated data after adding noise.**

## Abstract

Although the study of human trajectory anomalies is critical for advancing spatial data mining, empirical research remains severely hindered by a pervasive lack of ground-truth datasets. Despite the availability of several real-world and simulated human trajectory collections, these datasets exclusively capture normal mobility patterns and lack annotated anomalies. This specific scarcity is fundamentally driven by the inherent statistical rarity of anomalous events, precluding the feasibility of conventional observational methods. Compounding this challenge, the systematic acquisition of large-scale mobility data is strictly bottlenecked by prohibitive costs and stringent privacy regulations. To overcome these fundamental limitations and establish a reliable human trajectory anomalies dataset with annotated ground truth, we introduce a novel, end-to-end generative framework designed to synthesize realistic trajectory anomalies at scale. Our architecture bridges the gap between purely synthetic mobility data and complex real-world physical constraints by operating directly on baseline simulated trajectories. We employ Large Language Model (LLM) agents to systematically inject semantically meaningful behavioral anomalies such as irregular out-of-distribution check-ins and skipped routine visits. To ensure rigorous spatial validity, the system leverages map-constrained routing reconstruction to recalculate the physical transitions between these LLM agent-modified waypoints. Moreover, to narrow the simulation-to-reality gap, we augment the resulting trajectories with a context-aware spatial noise model, parameterized by environmental and location-specific variables, to accurately emulate heterogeneous GPS sensor degradation. Through this pipeline, the system generates high-fidelity, rigorously annotated mobility datasets that serve as a critical foundation for the robust evaluation of downstream spatial data mining systems.

## CCS Concepts

• Information systems → Geographic information systems; Location based services.

## Keywords

Trajectory Data, Anomaly Generation, Human Mobility, Noise Module, Large-Language Models

## 1 Introduction

The analysis of abnormal human mobility trajectory data is critical for diverse applications, including the quantification of POI popularity [6] and the evaluation of population dynamics during the COVID-19 pandemic [11, 28]. However, the widespread utilization of mobility data introduces substantial concerns; for instance, a patient may not want to publicly share visiting a clinic, and a student may not want to publicly share having skipped school. To mitigate these risks, empirical trajectory datasets are frequently subjected to data obfuscation techniques, specifically through the strategic deletion (skipping) and insertion (adding) of spatial-temporal records associated with selected locations. Because these deliberate synthetic modifications introduce structural deviations from empirically measured trajectories, the resulting altered sequences are often denoted as trajectory anomalies. [3, 29, 31].

Despite the proliferation of large-scale human mobility datasets from semantic point of interest (POI) check-ins (e.g., Gowalla [7], Foursquare [37], Massive-STEPS [35]) to raw continuous coordinate traces (e.g., GeoLife [40], T-Drive [39], Grab-Posisi [15], World-Trace [42]), existing empirical research on human trajectory anomalies remains severely constrained by a lack of ground-truth data. This profound discrepancy stems from the fundamental difficulty

of capturing anomalies in the wild. For instance, commercial ride-sharing trajectories [15, 39] inherently capture disjointed, task-driven passenger requests rather than continuous, individualized longitudinal mobility, rendering these datasets unsuitable for trajectory anomaly detection tasks. Similarly, volunteer-contributed logs are plagued by compliance fatigue and privacy concerns, yielding highly sparse and fragmented records with significant temporal gaps. For example, the widely used GeoLife dataset [40] includes trajectory data for only 182 individual users. Furthermore, while the Gowalla dataset [7] contains a total of 196,591 users and approximately 6,442,890 check-ins, the average number of check-ins per user is merely 32. While naturally occurring anomalous events undoubtedly exist within these massive observational collections, the extreme sparsity of continuous records and the complete absence of native ground-truth annotations render them fundamentally unusable for robust anomaly analysis. In addition, this structural scarcity is strictly inadequate for modeling long-term behavioral patterns, making it nearly impossible to reliably distinguish true anomalies from benign mobility variance or to benchmark detection algorithms. Furthermore, real-world data is frequently degraded by sensor noise, outdated POI mappings, and the inherent challenges of accurate semantic enrichment. Consequently, synthetic datasets generated in highly controlled environments have emerged as a preferred alternative for establishing reliable ground truth. Currently, only NUMOSIM [31] is explicitly designed to provide native labels for benchmarking abnormal behaviors. Yet, its practical utility is severely limited by its overly simplistic anomaly design. NUMOSIM's anomalies are confined to basic alterations—such as shifting a stay point's duration or inserting an unseen location—devoid of any causal reasoning as to why the anomaly occurred. In addition, NUMOSIM does not provide raw continuous trajectories alongside its discrete check-ins, it leaves a critical void in the benchmarking of continuous spatial anomaly analysis systems.

To overcome these fundamental limitations, this paper introduces a novel, cost-effective generative framework that leverages LLMs to synthesize realistic, high-fidelity trajectory anomalies at scale. Recognizing the structural isomorphism between natural language and human mobility, our methodology employs a persona-driven LLM acting as a "High-level Reasoning Agent" to analyze normative routines and intelligently inject contextually grounded, physically feasible deviations via Insert and Skip strategies, as illustrated in Figure 1. Furthermore, to mitigate the persistent challenge of LLMs hallucinating spatial coordinates, we introduce a robust three-stage translation architecture. By integrating stay point detection, highly accurate travel mode prediction, and map-constrained routing, this pipeline systematically converts semantic anomaly sequences into continuous, 0.2Hz raw GPS coordinate traces. Finally, to effectively close the simulation-to-reality gap, we apply a comprehensive, statistically grounded noise model to emulate complex real-world sensor imperfections.

Specifically, this paper makes the following contributions:

- (1) **Novel LLM-Driven Framework for Anomaly Synthesis:** We introduce a persona-driven anomaly generation framework that utilizes LLMs to analyze human mobility routines and intelligently inject contextual, non-trivial anomalies. The system employs targeted Insert, Skip and Detour strategies while strictly enforcing physical feasibility parameters to prevent spatiotemporal overlaps.
- (2) **Robust Translation from Semantic Sequences to Continuous Raw Coordinates:** To mitigate LLM spatial hallucination, we developed a three-stage conversion architecture. This includes a sequential based stay point extraction, a highly accurate decision tree-based travel mode predictor, and precision routing via Valhalla to generate continuous, 0.2Hz GPS coordinate traces that adhere to rigid transit schedules.
- (3) **Comprehensive Multi-Layered Noise Simulation for Sim-to-Real Transfer:** We designed a robust, multi-layered noise injection model to mimic real-world GPS imperfections and prevent model overfitting. This component rigorously simulates macro environmental atmospheric drift, micro environmental urban canyon multi-path scattering, and system-level signal dropouts, yielding a high-fidelity data with enhanced realism.

Our generated dataset based on SF-Life, perturbed by anomalies and noise, is available at <https://hf.co/datasets/spatialcomputing/SF-TPAN>

## 2 Background and Related Work

In this section, we review the existing literature and foundational concepts that inform our generative framework. First, Section 2.1 establishes the theoretical context by examining current definitions, taxonomies, and methodological approaches to human trajectory anomalies. Building upon this, Section 2.2 evaluates widely utilized human mobility datasets, detailing their collection methodologies, temporal coverage, and fundamental limitations regarding the provision of anomaly ground truth. To contextualize our synthetic methodology, Section 2.3 explores recent advancements in the application of LLMs for human mobility and trajectory generation.

### 2.1 Human Trajectory Anomalies

While an anomaly is generally defined as a data point that significantly deviates from a normative data distribution, the specific definitions of human trajectory anomalies vary considerably across studies. Consequently, rather than establishing a singular foundational definition, this section surveys recent geospatial literature to systematically categorize the diverse types of human mobility anomalies. Recent literature generally categorizes trajectory and mobility anomalies into five distinct paradigms based on spatial, temporal, semantic, and relational contexts.

- (1) **Sub-trajectory and Route Anomalies:** Anomalies frequently manifest as localized spatial deviations within a specific trip, rather than encompassing the entire trajectory. This classification is primarily composed of two structural types: detour anomalies and switch anomalies [17]. Detour anomalies occur when an agent navigates an unnecessarily elongated or alternative route, typically to avoid sudden roadblocks or unexpected traffic. Switch anomalies occur when multiple valid routes exist between a given source-destination pair and a trajectory initially follows one established normal route but abruptly switch to a completely different normal route in the middle of the trip. Addition anomalies include Time Anomalies, in which the travel speed of a trip is changes and Loop Anomalies in which loops from a location to itself are added.

- (2) **Individual Behavioral and Routine Anomalies:** Aligning with the most commonly understood definition of behavioral irregularities, these anomalies represent temporal and spatial deviations from an individual agent’s established historical “patterns of life” [3, 14]. Within this classification, an abnormality is strictly relative to the specific individual rather than a generalized population baseline. It fundamentally defines an anomaly as an instance where an agent visits a location they typically do not frequent or abruptly breaks a recurring schedule, such as an employee remaining at home during a standard workday.
- (3) **Contextual and Semantic Anomalies:** These anomalies are defined as structurally valid movements that only become anomalous when evaluated at the intersection of an agent’s specific identity, temporal variables, and the semantic category of the visited PoI [9]. The anomalous state of a trajectory is strictly conditioned upon the specific demographic or occupational role of the agent. For instance, highly localized, frequent neighborhood stops are perfectly normative for a door-to-door salesperson, but would be classified as highly anomalous if suddenly exhibited by an individual who historically works from home.
- (4) **Collective and Co-traveling Anomalies[34]:** This classification shifts the analytical focus from isolated agents to complex spatiotemporal dependencies and interactions among multiple individuals. A trajectory may appear normative individually but become highly anomalous when contextualized against the expected co-occurrence of social ties. Literature categorizes these interaction-driven deviations into three primary subtypes: unexpected co-occurrence anomalies, where agents share a location without historical precedent; absence anomalies, where an expected participant is missing from a joint event; and synthetic coordination anomalies, where historically isolated individuals artificially converge at a shared destination. For example, a student remaining at home during the evening exhibits normal individual behavior; however, being unexpectedly home alone while their parent is absent constitutes an anomaly.
- (5) **Kinematic and Physical Anomalies[19, 30]:** This classification defines an anomaly as a spatiotemporal sequence that violates fundamental physical laws or mechanical constraints, such as implausible acceleration or teleportation. In the context of human mobility, pure physical anomalies are exceedingly rare. Consequently, these deviations are primarily treated as issues of underlying data quality rather than reflections of actual human behavior. These impossible movements most frequently result from hardware device failures, signal degradation, or intentional adversarial manipulation, such as GPS spoofing.

## 2.2 Human Mobility Anomaly Datasets

In this section, we examine several prominent human mobility datasets.

Within the spatial data mining literature, human mobility datasets predominantly rely upon four distinct data representation frameworks: constant time intervals (CTI), variable time intervals (VTI), event-based intervals (EBI), and constant time periods (CTP) [21], with constant time intervals and event-based intervals being the most widely adopted.

**2.2.1 Constant Time Intervals (CTI) representations.** This representation methods consist of spatial coordinates, specifically latitude

and longitude, paired with exact timestamps at constant intervals. These trajectories are typically captured through GPS-enabled devices and theoretically represent a continuous and smooth movement path. This continuous format explicitly captures the moving object’s kinematic state at any given moment, including velocity, acceleration, and rate of turn.

YJMob100K[36] provides an extensive, longitudinal record of human mobility CTI formatted trajectories, capturing the movements of up to 100,000 individuals over a 75-day period within four metropolitan area. The raw location pings are severely discretized into 500-meter by 500-meter spatial grid cells and 30-minute temporal bins. While the dataset includes a 15-day subset captured during an undisclosed emergency, it entirely lacks the explicit, ground-truth anomaly labels required for training and benchmarking supervised trajectory anomaly detection models.

Unlike purely observational datasets, Urban Anomalies [3] is generated via an agent-based Pattern of Life simulation. It uniquely provides data in both continuous raw coordinate formats and discrete semantic representations, encompassing staypoints and check-ins. To establish explicit ground-truth labels for benchmarking, the framework systematically injects predefined behavioral deviations across four distinct categories: increased feeding frequency, altered recreational preferences, randomized recreational site selection, and occupational absenteeism.

Despite providing native ground-truth annotations, the dataset exhibits limitations regarding physical realism. Because the underlying simulation assumes constant-speed movement along strict shortest-path routes, the resulting raw trajectories fail to capture true real-world kinematic variances, such as speed limit, localized traffic congestion. Furthermore, the injected outliers are strictly constrained to four types of behavioral scheduling rather than complex spatial routing anomalies (e.g., physical detours). Consequently, these abnormal deviations lack structural spatial complexity, allowing them to be trivially identified using classic anomaly detection algorithms[26].

**2.2.2 Event-Based Intervals (EBI) Representations.** Event-Based Intervals representations provide a higher-level abstraction of mobility, where a continuous trajectory is discretized into a chronological sequence of stay points. Rather than passively logging raw physical coordinates, this format effectively functions as a targeted check-in table restricted to a limited set of PoI locations. These discrete points are usually enriched with contextual and semantic metadata, explicitly identifying the functional purpose of the location alongside precise arrival and departure timestamps. While semantic sequences are highly effective for modeling normative human behavior, real-world observational datasets fundamentally lack explicit ground-truth anomaly annotations. Currently, NUMOSIM [31] stands as the exclusive EBI formatted trajectory dataset equipped with explicit ground-truth annotations for anomaly detection. Comprising synthetic mobility records for 200,000 agents over an 8-week period in Los Angeles, the dataset models abnormal behaviors by strategically injecting behavioral deviation. Specifically, it introduces two primary categories of anomalies: altered stay points: characterized by temporal shifts in arrival or departure times, and inserted stay points: which representing novel spatial visits not observed during the training phase. Additionally, this

dataset is enriched with agent demographic profiles and detailed PoI metadata.

### 2.3 LLM-based Human Trajectory Generation

Recently, the rapid advancement of LLMs has opened new avenues for human mobility generation, overcoming the semantic and interpretability limitations of traditional deep generative models. Existing frameworks employ diverse input representations and reasoning strategies to simulate mobility.

In the Geo-Llama[23] framework, the LLM is fine-tuned for trajectory generation by formulating the task as a next-token prediction problem, encoding input trajectories as standardized text strings. Conversely, MobGLM[38] using multimodal tokens that represent demographic attributes, location zones, activity types, and transportation modes. CAMS[8] generates trajectories by utilizing user demographic profiles, regional summaries, and historically activity sequences as inputs. TrajLLM[18] iteratively predicts the next logical semantic activity using demographic data, personality traits, PoIs, and historical routines. Finally, LLMob[32] incorporates personas, specific contextual prompts, and historical data, utilizing retrieval-augmented reasoning to infer daily motivations and combine them with identified habitual activity patterns to generate daily activity trajectories.

A primary challenge in LLM-driven spatial generation is validating outputs and mitigating spatial hallucinations (e.g., physically implausible or topologically incorrect) While various mechanisms exist to address this, they differ across models. For example, Geo-Llama[23] relies on a post-processing integrity check to resolve physical impossibilities. CAMS[8] addresses geographic hallucinations by tracking the Toponym Valid Ratio metric, utilizing fine-grained POI data, and employing hierarchical address representations. MobGLM[38] avoids generating fake coordinates by confining the spatial generation to predefined administrative small zone codes and measures sequence validity using automated metrics like LCSS, BLEU, and ROUGE-L. TrajLLM[18] prevents spatial inaccuracies by strictly limiting LLM-based recommendations using real POI data and historical visit frequencies. LLMob[32] scores the generated patterns by comparing them against real-world trajectories to ensure consistency.

Despite these mitigation strategies, LLM hallucination remains a significant challenge in ensuring spatial validity. Consequently, the majority of current models predominantly generate semantic or check-in-level records rather than fine-grained, raw trajectory data. Furthermore, the advancement of this domain is constrained by data accessibility, as several of the datasets utilized in existing literature remain closed-source.

## 3 Methodology

To address the scarcity of labeled anomaly data in spatial-temporal domains, we propose a novel end-to-end framework for synthesizing anomalous trajectories that accommodates dual-format datasets comprising both CTI and EBI. In this section, we detailed the deployment of an LLM as the spatial-temporal anomaly generator. By leveraging the reasoning capabilities of the LLM, the framework can synthesize three of the five anomaly typologies defined in Section 2.1. The generation pipeline partitions the workload based on the specific structural requirements of each anomaly

class: a Valhalla routing engine[1] computes the Sub-trajectory and Route Anomalies while also providing interpolation for injected POIs, whereas the LLM directly formulates the Individual Behavioral and Routine Anomalies, as well as the Contextual and Semantic Anomalies. In addition, to mitigate LLM spatial hallucinations and overcome the sparsity of traditional check-in records, our approach implements a dual-stage generation mechanism: PoI-level map matching and continuous, second-by-second raw trajectory synthesis. The whole framework is shown in Figure 2, which includes four components: Data Preprocessing, LLM-Driven Anomaly Generation, Hallucination Mitigation, and Post Processing for raw trajectory synthesis. Furthermore, to the best of our knowledge for the first time, we provide a noise model to enhance realism during the raw trajectory synthesis, enabling the precise generation of the distinct anomaly typologies defined in the related work.

### 3.1 Data Ingestion and Preprocessing

The data ingestion and preprocessing pipeline transforms raw tabular mobility data into a structured textual format optimized for LLM processing. The framework initially ingests the SF-Life[2] dataset check-in record part and Foursquare NYC [37] data. To minimize memory overhead and maximize computational efficiency, the ingestion module selectively extracts the five essential features required for spatiotemporal modeling: User ID, Timestamp, Latitude, Longitude, and PoI Category. Let  $U = \{u_1, u_2, \dots, u_{|U|}\}$  denote the set of users. For a specific user  $u \in U$ , a raw spatial-temporal trajectory is defined as a chronologically ordered sequence of check-in events, denoted as:  $T_u = \langle e_1, e_2, \dots, e_n \rangle$ . Each event  $e_i$  is represented as a tuple  $e_i = (t_i, c_i, l_i)$ , where:  $t_i$  is the chronological timestamp.  $c_i$  is the categorical Point of Interest (POI) string.  $l_i = (\phi_i, \lambda_i)$  represents the spatial coordinates, consisting of latitude  $\phi_i$  and longitude  $\lambda_i$ . Given that LLMs operate on textual inputs, the tabular trajectory data is subsequently mapped into a continuous semantic representation. The dataset is grouped by User ID, and each individual check-in event is serialized into a strict, standardized formatted textual string:  $s_i = t_i|c_i|@|\phi_i, \lambda_i$ , where '|' is a delimiter. The final semantic trajectory for user  $u$ , denoted as  $S_u$ , is constructed by concatenating the ordered sequence of strings  $\{s_1, s_2, \dots, s_n\}$  using a newline delimiter character sequence. Furthermore, leveraging the comprehensive metadata available within the simulated SF-life dataset, we integrate agent demographic profiles into the modeling pipeline. This demographic context includes the agent's age, gender, home location, and occupational category.

### 3.2 LLM-Driven Anomaly Generation

Our framework employs an LLM to synthesize Individual Behavioral and Routine Anomalies, along with Contextual and Semantic Anomalies. To execute these tasks, we develop an agentic architecture that summarizes historical agent trajectories and subsequently plans the spatial coordinates and abnormal behavioral patterns of the deviations. Prioritizing computational efficiency and cost optimization, the system omits locally deployed architectures and spatially trained, domain-specific models. Instead, we adopt GPT-5-mini as the foundational reasoning engine to drive the trajectory generation process.

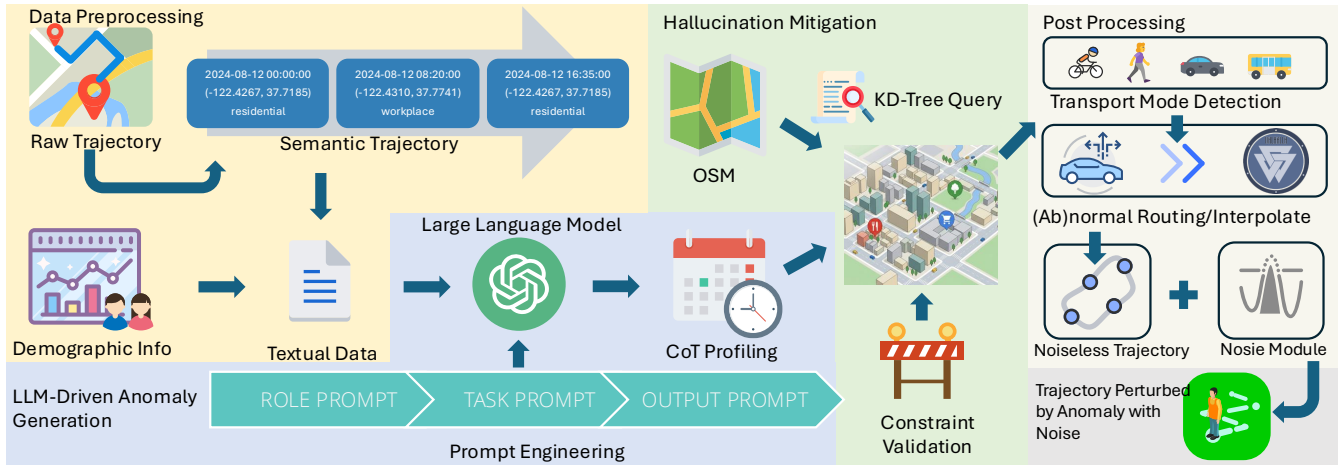


**Figure 2: The Illustration of Our Framework for Synthesizing Anomalous Trajectories. (Left) Data Preprocessing; (Middle Lower) LLM-Driven Anomaly Generation; (Middle Upper) Hallucination Mitigation; (Right) Post Processing.**

**3.2.1 Prompts Engineering.** Given that GPT-5-mini operates as a general-purpose language model rather than a specialized geospatial engine, rigorous prompt design is essential to adapt its capabilities for spatiotemporal anomaly synthesis. To maximize the accuracy and reliability of the synthesized outputs, we engineered a systematically structured prompt[13] ensures the model correctly parses complex trajectory sequences and fully comprehends the defined anomaly generation objectives. Specifically, the prompt architecture is systematically partitioned into four functional components: role assignment, task definition, critical constraints, and output schema. Initially, in the role assignment part, we define the operational bounds by assigning the LLM a specialized persona restricted to a predefined spatial and temporal domain. Within this part, we also explicitly define two categories of anomalies. During the task definition phase, we direct the model to profile the baseline routine of the agent prior to formulating a minimum of five distinct anomalies. Specifically, the LLM classifies the overarching mobility archetype of the agent (e.g., a traditional corporate commuter or a university student) by evaluating the input trajectory sequence alongside the provided demographic data. Because anomalies rely strictly on the intersection of spatial events with agent identity or historical patterns, we impose a profiling requirement to establish a routine baseline. This baseline ensures that subsequent deviations represent genuine behavioral shifts rather than random spatial noise.

Following this profiling step, we require the model to design at least five distinct anomalies per agent based on. These spatiotemporal perturbations are executed by explicitly instructing the model to combine two primary disruption operations: Insert and Skip. The operational definitions of these strategies are detailed in Table 1, and two representative samples are illustrated in Figure 1. LLMs were excluded from generating Detour instructions due to context window limitations and a high susceptibility to spatial hallucinations (Section 3.2.2). Furthermore, because perturbation strategies alter required travel distances, transit times, and transportation modes, the Valhalla routing engine is employed to compute physically feasible waypoints. To prevent topologically or temporally

implausible trajectories, rigorous constraints are integrated into the prompt. The model must calculate insert windows strictly within existing temporal gaps, ensuring sufficient visit durations without causing event overlaps. Finally, to maintain a realistic temporal distribution, anomalies may span adjacent days but are strictly prohibited from being concentrated on a single calendar day.

**Table 1: Comparison of Trajectory Modification Strategies**

Strategy	Operational Characteristics
<b>Insert</b>	<p><b>Mechanism:</b> Synthesizes and injects an out-of-context check-in event into the timeline.</p> <p><b>Spatial Target:</b> Introduces an entirely novel POI or recontextualizes a previously visited coordinate.</p> <p><b>Temporal Constraint:</b> Must fit within an existing temporal gap; requires strict travel-time validation to prevent chronological overlaps.</p>
<b>Skip</b>	<p><b>Mechanism:</b> Deletes a highly predictable, habitual check-in event from the historical sequence.</p> <p><b>Spatial Target:</b> Removes an expected spatial coordinate without introducing new geographic data.</p> <p><b>Temporal Constraint:</b> Expands an existing temporal gap or transit time; avoids overlapping conflicts.</p>
<b>Detour</b>	<p><b>Mechanism:</b> Utilizes the Valhalla routing engine to create physically feasible intermediate waypoints.</p> <p><b>Spatial Target:</b> Produces a sequence of geographic coordinates that represent the adjusted travel trajectory and corresponding transportation mode.</p> <p><b>Temporal Constraint:</b> Recalculates required transit durations between dynamically altered check-in locations to maintain chronological integrity and physical viability.</p>

**3.2.2 Mitigation of Spatial Hallucinations.** A fundamental limitation of utilizing LLMs for geospatial tasks is their propensity for spatial hallucinations. This phenomenon occurs when the model generates highly plausible but entirely fictitious locations, non-existent POI, or topologically impossible coordinates [33].

To resolve this vulnerability and prevent physically impossible transitions, such as teleportation, our framework decouples the semantic intent of the anomaly from its precise geographic instantiation. First, rather than permitting the LLM to output arbitrary textual location names or raw coordinates, the prompt schema restricts the model to generating deterministic geographic search parameters. Specifically, the LLM must output a localized geographic search center, a bounding radius, and categorical OpenStreetMap (OSM) tags. A subsequent deterministic map-matching module executes this spatial query against the verifiable OSM database to retrieve an actual, existing POI. By anchoring the semantic reasoning of the language model to a rigorous geospatial database, this mechanism ensures that every generated anomalous location physically exists and is topologically valid, thereby neutralizing the risk of spatial hallucinations.

Second, we integrate a Chain-of-Thought (CoT) reasoning framework directly into the generation pipeline to mitigate hallucinations [4, 24]. Instead of executing zero-shot trajectory modifications, the model is required to decompose the anomaly generation task into a sequence of logical deductions. Before defining any executable abnormal generation commands, the LLM must first articulate the established behavioral persona of the agent, isolate the specific chronological pattern targeted for disruption, and explicitly calculate the available temporal insert windows between sequential check-ins.

**3.2.3 Bounding LLM Output for Automated Processing.** To guaranty seamless integration into automated processing pipelines and prevent the generation of extraneous conversational text, the framework constrains the LLM to a strict JSON output schema. By embedding concrete output exemplars directly within the system prompt, we strictly bound the model's generative behavior to a predefined structural format. This structural enforcement bypasses the parsing failures common to unstructured text, facilitating reliable and deterministic data extraction for downstream evaluation.

### 3.3 Raw Trajectory Synthesis

While LLMs are utilized to generate continuous mobility trajectories, they frequently fail to capture fine-grained spatial-temporal details[41] and introduce inherent movement uncertainty[12]. To overcome these limitations and ensure the generation of strictly valid raw trajectories, the framework employs the Valhalla routing engine. Following the derivation of the semantic anomaly parameters, Valhalla is utilized to synthesize the high-resolution, point-to-point coordinate sequences. To establish the transportation method between sequential POIs, the routing engine dynamically determines the travel mode and speed by evaluating key spatio-temporal constraints and agent demographics. For example, younger agents may prefer public transit rather than auto. Once the optimal travel mode is classified, the Valhalla engine computes the detailed sub-trajectories and routes the anomalous deviations. To guaranty the temporal and spatial accuracy of public transportation routes, we integrate SFMTA General Transit Feed Specification (GTFS) data directly into the routing infrastructure. Furthermore, the routing engine is explicitly parameterized using the demographic profile of the agent. By mapping demographic attributes to kinematic constraints and transit preference, the system algorithmically adjusts transit

metrics, specifically modulating travel speeds, travel mode preference. This comprehensive integration ensures that the synthesized raw trajectories adhere strictly to real-world transit schedules and the physical capabilities of the simulated agent, thereby preserving the structural realism and kinematic validity of the final mobility dataset. Crucially, as the Valhalla routing engine translates these LLM perturbations into raw trajectories, it must calculate specific Detour waypoints to accommodate the modified spatial dynamics. These waypoints ultimately manifest as the physical sub-trajectory and route-level anomalies.

### 3.4 Noise Module

To rigorously bridge the "sim-to-real" gap and mitigate algorithmic overfitting, we introduce a hierarchical synthetic mobility noise generation module. This module systematically injects realistic, physically grounded noise into ground-truth trajectories across three distinct environmental strata: the macro-environment, the micro-environment, and the receiver system. Given the absence of definitive empirical baselines for these noise parameters, their scaling factors are heuristically calibrated via qualitative visual inspection to ensure the resulting spatial deviations remain physically plausible.

**3.4.1 Macro-Environment Noise.** The first layer accounts for continuous atmospheric drift governed by time and meteorology. We quantify tropospheric interference using the Saastamoinen delay model [22, 27], which incorporates the zenith delay alongside a simple geometric mapping function. Leveraging historical ERA5 weather telemetry [5], the Zenith Hydrostatic Delay (*ZHD*) and Zenith Wet Delay (*ZWD*) are defined as:

$$ZHD = \frac{0.0022768 \cdot P}{1 - 0.00266 \cdot \cos(2\phi) - 0.00028 \cdot H}$$

$$ZWD = 0.0022768 \cdot \left( \frac{1255}{T} + 0.05 \right) \cdot e_s$$

$$SPD = (ZHD \times M_h(\epsilon)) + (ZWD \times M_w(\epsilon))$$

where  $P$  is the surface pressure,  $\phi$  is the latitude, and  $H$  is the altitude. The variable  $T$  represents the 2-m air temperature, and  $e_s$  denotes the vapor pressure, which is computed using the 2-m dewpoint ( $T_d$ ). To calculate the Slant Path Delay (*SPD*), we apply the hydrostatic mapping function ( $M_h(\epsilon)$ ) and the wet mapping function ( $M_w(\epsilon)$ ). Concurrently, signal propagation is subjected to an ionospheric delay ( $I$ ), modeled using the established ionospheric delay algorithm [20]:

$$I = \frac{40.3 \cdot 10^{16} \cdot TEC}{f_{L1}^2}$$

where  $TEC$  represents the Total Electron Content [16], and  $f_{L1}$  is the GPS  $L1$  signal frequency. To simulate the continuous temporal evolution of these atmospheric dynamics, the combined delay is formulated as a Gauss-Markov AR(1) process[10]. Given a data sampling interval  $\Delta t$ , a relaxation time constant  $\tau = 300$  s, and a decay factor of  $\phi = 0.82$ , the sequential delay state  $X_i$  updates recursively:

$$X_i = e^{-\frac{\Delta t}{\tau}} \cdot X_{i-1} + \mathcal{N}(0, [(SPD_i + I_i)]^2)$$

**Table 2: Quantitative Overview of Anomaly Injection and Spatial Mapping.**

Dataset	Planned Insert Number	Planned Skipped Number	OSM Mapped Number	Median Insert Radius (m)
SF-Life	368	203	337	324.03
Foursquare NYC	360	263	222	569.68

**Table 3: Demographic Classification Performance across Agent Types**

Agent Type	Total Number	Predicted Precision	Predicted Recall	Predicted $F_1$ Score
Homemaker	23	0.6154	0.3478	0.4444
Student	23	1	0.7826	0.8780
Worker	54	0.7246	0.9259	0.8130
<b>Average</b>		0.780	0.6854	0.7118

**3.4.2 Micro-Environment Noise.** The second layer models the multi-path noise inherent to dense urban infrastructure. To model the multi-path scattering effects characteristic of dense urban infrastructure, we inject localized positional noise governed by a zero-mean Laplace distribution[25]:  $f(\epsilon_{mp,i}; b_i) = \frac{1}{2b_i} \exp(-|\epsilon_{mp,i}|/b_i)$ . To dynamically modulate this interference based on spatial topology, we leverage structural footprint geometries extracted from OSM. For any given ground-truth receiver state  $X_i$ , we compute the minimum Euclidean distance  $d_i$  to the nearest building polygon. We establish a 15-meter proximity buffer to quantitatively delineate the urban canyon boundary. For open environments, the scale parameter  $b_i$  is set to 3; when a trajectory intersects the urban canyon buffer, it scales to 15 to emulate severe signal scattering.

**3.4.3 Receiver System Noise.** The final layer models endogenous receiver hardware anomalies and exogenous severe signal blockages. Thermal interference within the hardware is represented as standard Gaussian noise with a standard deviation of  $\sigma = 1.5$ . To simulate severe signal blockages, complete dropouts, or momentary receiver failures caused by physical obstructions, we implement a dynamic masking function governed by a Poisson process. Let  $M_i$  denote the binary availability mask at epoch  $i$ , where the masking probability is dictated by the threshold parameter  $\lambda$ . The probability mass function for the underlying Poisson event occurrences  $k$  is given by:  $P(k; \lambda) = \frac{\lambda^k e^{-\lambda}}{k!}$ , such that a blockage occurs ( $M_i = 1$ ) when  $k > 0$ . The active signal input mask threshold  $\lambda$  is dependent upon the physical environment, specifically open conditions versus highly obstructed topologies, such as tunnels. During intervals of active signal loss, we model these severe positional anomalies,  $c_i$ , by sampling from a heavy-tailed Cauchy distribution:  $f(c_i; x_0, \gamma) = \frac{1}{\pi\gamma[1+((c_i-x_0)/\gamma)^2]}$  where the location parameter  $x_0$  is centered at 0, and the scale parameter  $\gamma$  is aggressively set to 15 to simulate the heavy tails characteristic of complete signal degradation.

## 4 Experimental Results and Analysis

In this section, we detail the experimental settings utilized to rigorously evaluate the spatial fidelity and kinematic plausibility of the generated synthetic abnormal trajectories.

To rigorously evaluate the efficacy of our proposed synthetic anomaly generation framework, we conduct extensive experiments leveraging two distinct spatial-temporal datasets: SF-Life dataset and Foursquare NYC dataset. To ensure a balanced and computationally tractable evaluation, we isolate a representative cohort of 100 unique users from each respective dataset.

### 4.1 Datasets and Preprocessing

SF-Life is a large-scale simulated mobility corpus designed to advance transportation and machine learning research, serving as our primary simulated environment. Over a 70-day observation period, the dataset provides complete, noise-free, multi-modal trajectories for 500,000 agents within the San Francisco Bay Area. It is characterized by a dual-modality structure comprising both discrete check-in records and continuous raw trajectories, supplemented by complete agent demographic data and localized building maps.

Foursquare NYC is utilized to validate the framework’s performance on real-world, sparse mobility data. Collected over approximately 10 months, this dataset comprises 227,428 discrete user check-ins within New York City. Structurally, each data point is defined by its spatial-temporal coordinates and is augmented with a discrete semantic label representing the granular category of the visited venue.

**4.1.1 Data Processing and Prompt Serialization.** To operationalize the raw tabular check-in data for LLM inference, we implement a deterministic serialization pipeline, detailed in Section 3.1, which maps discrete spatial-temporal records into structured context windows. To optimize token utilization and maximize the effective context length of the LLM, the continuous spatial coordinates  $(\phi, \lambda)$  are quantized to a precision of four decimal places. This lexical quantization preserves sufficient spatial resolution for micro-level urban mobility modeling while significantly reducing token overhead. Subsequently, user demographic information, such as age and occupation, is embedded into the user prompt payload alongside the concatenated trajectory  $\mathcal{S}_u$  and a predefined system prompt specifying the anomaly generation heuristics.

Given the coarse-grained categorical structure of the SF-Life dataset, which contains only five discrete POI classes, we constrain the LLM’s generative output. Instead of prompting the model to predict specific OSM spatial venues, we require it to deterministically select from a predefined set of categorical labels.

**4.1.2 Dataset Configuration.** For the SF-Life dataset, to ensure computational tractability, our experiments utilize a subset comprising 100 distinct agents. Trajectories within this dataset are sampled at a high-frequency temporal resolution of 5 seconds, yielding approximately  $1.2 \times 10^6$  coordinate points per agent. For the Foursquare NYC dataset, we filter the data to extract a representative cohort consisting of the top 100 most active unique users.

**4.1.3 Perturbation Variants.** To benchmark the proposed anomaly generation framework, we construct six distinct perturbation variants for the SF-Life dataset: **Insert-only**, **Skip-only**, **Insert with noise**, **Skip with noise**, **combined Insert and Skip**, and **combined Insert with Skip and noise**. To comprehensively evaluate the efficacy of our proposed anomaly generation framework, we benchmark its performance against two baseline:

**Table 4: Evaluation of Generated Abnormal Trajectories Across Perturbation Variants.**

Trajectory Perturbation Variant	Evaluation Metrics					
	Kinematic Violation Rate	Dwell-Time Shift (s)	Spatial Novelty Ratio	Normalized FastDTW Deviation Cost (m)	Centroid Shift Distance (m)	Temporal Retention Rate
Insert	0.0053	-1.7082	0.0274	4.7207	6.7733	1.0000
Skip	0.0050	1.1762	0.0257	8.9523	15.4753	1.0000
Insert w/Noise	0.4260	-5929.4957	0.2093	34.0098	6.8082	1.0000
Skip w/Noise	0.4160	-5931.2831	0.2079	43.1483	15.5058	1.0000
Insert+Skip	0.0052	-0.4581	0.0275	12.1071	14.9140	1.0000
Insert+Skip w/Noise	0.4258	-5933.9265	0.2095	48.3594	14.9200	1.0000
Linear Interpolation Baseline	0.0003	5714929.7163	0.0786	14.1236	17.0865	0.9663
Co-location Swap Baseline	0.0052	-0.0001	0.0603	81.7863	74.1249	1.0000

- (1) **Linear Interpolation Baseline:** This approach constructs synthetic trajectories from discrete check-in records. It first isolates stationary events to calculate the temporal transit durations between consecutive POI. A spatial trajectory is then generated by applying linear interpolation between these POI.
- (2) **Co-location Swap Baseline:** Beginning on the 30th day of the observation window, the algorithm identifies pairs of agents exhibiting spatial-temporal co-location. Upon detecting an intersection, the subsequent trajectory sequences of the co-located agents are swapped.

Conversely, because the Foursquare NYC dataset consists of discrete check-in records lacking raw, high-frequency trajectory data, we restrict its anomaly generation exclusively to the combined Insert + Skip variant. A quantitative overview of the LLM anomaly injection and spatial mapping metrics is list in Table 2. SF-Life dataset demonstrates a higher OSM mapping success rate, successfully grounding 337 of 571 planned insertions compared to 228 for Foursquare NYC. Additionally, the Foursquare NYC anomalies exhibit significantly greater spatial dispersion, indicated by a median insertion radius of 569.68 meters versus 324.03 meters for the SF-Life dataset. To validate the LLM’s capability to deduce agent occupations and underlying behavioral patterns from mobility trajectories, Table 3 shows its demographic classification performance on the SF-Life dataset. It demonstrates that LLM have a high proficiency in identifying extract and classify rigid, predictable occupational patterns like students and workers with a  $F_1$  score of 0.87 and 0.81. However, the model exhibits a significant performance degradation with highly variable, unstructured daily trajectories like homemakers ( $F_1$  score: 0.44).

## 4.2 Evaluation Metrics

To rigorously validate the quality of the synthesized dataset regarding kinematic plausibility and spatial validity, we augment qualitative visual inspections of selected trajectories with six quantitative evaluation metrics. As these structural computations necessitate continuous high frequency coordinate sequence, we restrict their application exclusively to the SF-Life dataset.

**Kinematic Violation Rate (KVR):** evaluates the physical plausibility of the generated trajectory  $T$  by analyzing the instantaneous velocity between consecutive points. It measures the proportion of spatial-temporal transitions that exceed the agent’s maximum dynamic speed threshold,  $v_{\max}$ , relative to the original trajectory.

**Dwell-Time Shift (DTS):** This metric evaluates the temporal stationarity of the modeled agent by quantifying the discrepancy in total stopping duration between the generated and original trajectories. In our case, an agent is considered dwelling if its instantaneous velocity  $v_t$  falls below a dynamic dwell-speed threshold,  $v_{\text{dwell}}$ . This metric will quantifies whether the synthetic trajectory includes excessive stationary periods compared to the original.

**Spatial Novelty Ratio (SNR):** This metric evaluates the efficacy of spatial anomaly injection by quantifying the proportion of newly explored geographical space. We discretize the agent’s routine mobility footprint into a 100x100 spatial heatmap, defining  $\mathcal{G}_{\hat{T}}$  as the set of all populated grid cells derived from the ground-truth sequence  $\hat{T}$ . The SNR computes the fraction of trajectories in the generated trajectories  $T$  that fall either entirely outside the original bounding box or within historically unvisited grid cells.

**Normalized FastDTW (NDTW):** This metric quantifies the absolute spatial divergence between the generated trajectory and the ground-truth sequence. We explicitly exclude point-to-point metrics, such as Mean Distance Error, because our perturbation methodology introduces abnormal scheduling.

**Centroid Shift Distance (CSD):** This metric evaluates the macro-level geographic stability of the synthetic trajectory. A minimal Centroid Shift indicates that the injected anomaly functions as a realistic, localized detour. Conversely, a substantial shift signifies a long-distance spatial displacement, rendering the manipulated trajectory easily identifiable by standard anomaly detection models.

**Temporal Retention Rate (TRR):** TRR quantifies structural preservation by calculating the ratio between the cardinality of the generated synthetic trajectory  $T$  and the original ground-truth trajectory  $\hat{T}$ . This metric assesses frameworks that incur data loss from sampling, temporal masking, or sequence skipping.

## 4.3 Quantitative Experimental Results

The metrics evaluation results are shown in Table 4, the un-noised variants (Insert, Skip, and Insert+Skip) maintain an exceptionally low KVR, ranging from 0.0050 to 0.0053. This performance is comparable to the Agent Swap baseline (0.0052), validating that the proposed insertion and skipping modifications preserve the physical plausibility of the original motion profiles without introducing unrealistic teleportation artifacts. Conversely, the noised variants exhibit an elevated KVR (0.4160 to 0.4260) strictly due to coordinate jittering. The Linear interpolation baseline yields the lowest KVR, which is a direct consequence of the shortened travel distances

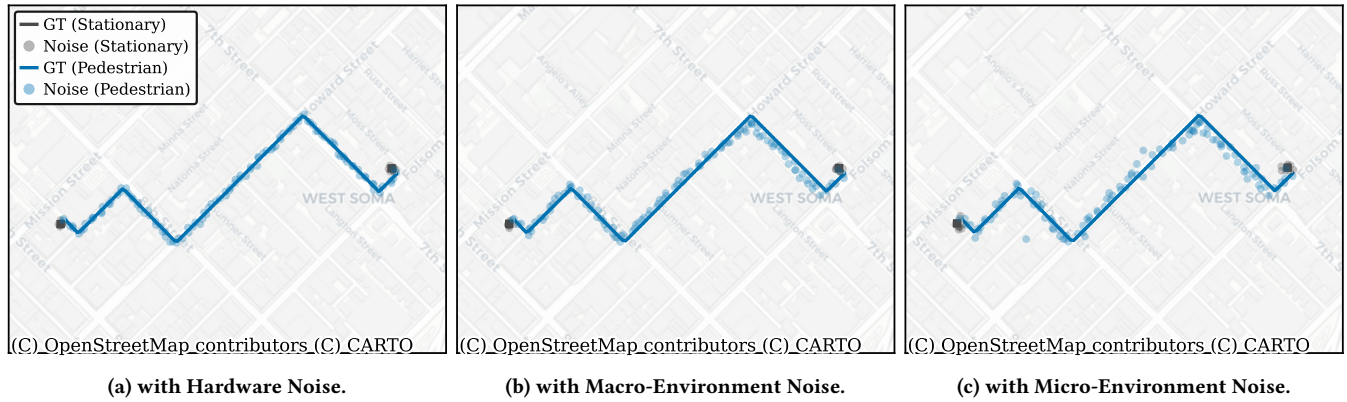


**Figure 3: Visualization of the three distinct noise layers added to the raw data: (a) hardware noise, (b) macro-environment noise, and (c) micro-environment noise.**

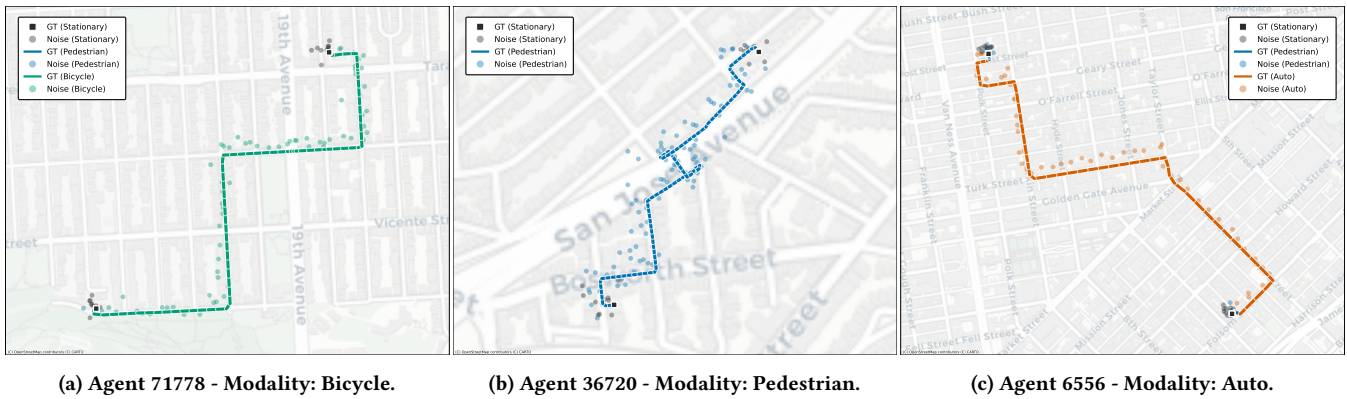


**Figure 4: Examples of trajectory modification under varying behaviors. The plots display noised agent trajectories across different travel modes and travel distances.**

inherent to straight line path interpolation. All our proposed perturbation variants achieve a TRR of 1.0, which confirms that our generation pipeline strictly maintains perfect temporal alignment with the original trajectories, providing none dropout. For the DTS metric, un-noised variants exhibit minimal temporal shifting, ranging from -1.7082 s to 1.1762 s. This indicates that despite executing multiple insertion and skipping operations, the methodology retains high fidelity in preserving the agent’s total stopping duration. In contrast, the noised variants induce a severe temporal shift. This is an expected artifact, as coordinate fluctuations introduced by the noise model are erroneously registered by the metric as continuous spatial drift rather than stationary periods. In the SNR metric, Un-noised variants witnessed a controlled, localized deviations, yielding light SNR increases. While the noised variants increasing the SNR to approximately 0.209. This behavior satisfies the requirement for generating prominent spatial anomalies while preserving a realistic overall trajectory structure by preventing the excessive inclusion of unvisited geographic regions. Regarding geometric similarity, the Insert variant yields a low NDTW cost of 4.7207 m, escalating to 8.9523 m for the Skip variant, and reaching 12.1071 m under the combined configuration; Meanwhile the noised variants increases the NDTW to 48.3594 m. Furthermore, the CSD metric demonstrates that both the Insert and Skip variant successfully minimize global spatial displacement, bounding the deviation to

strictly under 20 m. This cumulative alignment cost confirms that the constituent perturbation methods operate independently, while the LLM provide non-overlapping distortion instruction during the inference phase. Overall, this adherence to the minimal distortion principle verifies that the synthesized anomalies function as realistic, highly localized detours.

Regarding the baseline, Co-location Swap Baseline incurs an immense NDTW cost of 81.7863 m. Considering this perturbation was restricted to only ten agent pairs, the magnitude of this error at the individual trajectory level is exceptionally high. For the Linear Interpolation Baseline, deviations are constrained because the interpolation strictly targets transit segments, which constitute a very limited fraction of the dataset. The CSD results also corroborate this, indicating that altering only transit segments does not fundamentally distort the overarching trajectory anchors. However, the massive displacement observed in Co-location Swap and the transit artificiality of the linear interpolation reveal that these methods cause an unnatural, global migration of the agent’s fundamental mobility patterns. Such structural artifacts render these baseline trajectories easily detectable by standard anomaly detection models.

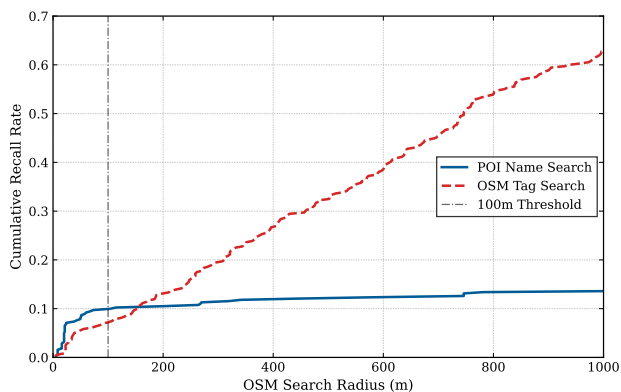


Figure 5: Cumulative Recall Rate for Name or Tag Search.

#### 4.4 Qualitative Experimental Results

We conducted a qualitative visual inspection on several generated anomalies to verify structural and physical plausibility. Visual evidence from Figure 1 demonstrates the framework’s capability to seamlessly execute behavioral modifications. In the insertion scenarios, the synthetic trajectory successfully diverges from the original POI A to incorporate the newly inserted POI B without exhibiting unnatural discontinuities or sudden spatial jumps (“teleportations”) while adhering to physical constraints of the road network. Similarly, for skip modifications, the generated trajectory excludes the skipped trip to and from Location B and creates a new trajectory directly from A to C that, qualitatively, appears difficult to discriminate from any trajectory originally found in the dataset.

#### 4.5 Noise Module Evaluation

Figure 3 illustrates the noise module described in Section 3.4 progressively compounding impact of hardware, macro-environment, and micro-environment noise, which collectively introduce severe spatial variance and anomalies to the trajectory. Figure 3a isolates the baseline hardware noise, where positional deviations remain minimal and tightly clustered along the ground truth. Figure 3b introduces atmospheric delays derived from weather data[5, 16] and AR(1) drift to this baseline; the AR(1) process causes consecutive data points to maintain correlated error vectors, systematically pulling the recorded trajectory off-center rather than generating uniform, uncorrelated scatter. Finally, Figure 3c demonstrates the severe trajectory degradation characteristic of dense urban environments through the injection of heavy-tailed micro-environmental noise, which results in extreme positional outliers. Building upon this, Figure 4 validates the noise model across bicycle, pedestrian, and automobile modalities, demonstrating an inverse relationship between agent velocity and trajectory degradation. Specifically, the low-velocity pedestrian modality (Figure 4b) exhibits severe relative spatial variance because time-correlated and localized multipath errors accumulate densely over short distances. Conversely, the high-velocity automobile trajectory (Figure 4c) maintains a smoother observed path. As the plotted trajectories demonstrate, the proposed framework generates realistic, spatially heterogeneous noise. This methodology surpasses conventional approaches by successfully mitigating the unrealistic uniformity and detectable artifacts characteristic of spatially homogeneous noise.

#### 4.6 Comparison Studies

To evaluate the spatial hallucination mitigation method discussed in Section 3.2.2, we evaluated this approach against a baseline that prompts for direct location names while keeping all other prompt parameters constant. Both methods were assessed using a search function to determine their ability to map generated outputs to real-world locations. As illustrated in Figure 5, empirical results demonstrate that direct POI name generation yields a spatial resolution accuracy of approximately 10% at a strict 100 m distance threshold. This accuracy marginally plateaued at 13% even when the search radius was expanded to the 1 km limit. In contrast, the proposed tag-based search strategy achieved a cumulative recall rate of 60%. These findings confirm that the generation of OSM tags rather than exact POI names significantly mitigates spatial hallucinations in LLMs. By constraining the generation space to standardized spatial metadata instead of discrete entity identifiers, our proposed methodology enhances factual grounding and spatial retrieval accuracy.

#### 5 Conclusions and Future Work

In this paper, we propose a novel end-to-end generative framework to address the critical scarcity of annotated GT data in human trajectory anomaly research. This framework provides a scalable mechanism to synthesize high-fidelity annotated mobility datasets for the robust evaluation of downstream tasks. By leveraging a person mobility pattern and demography enabled LLM, the framework systematically injects contextually grounded and physically feasible deviations into normative mobility routines via Insert, Skip and Detour operations. To mitigate the LLMs spatial hallucination, we designed a robust three-stage translation pipeline. This pipeline integrates sequential stay point extraction, demography based travel mode prediction, and map-constrained routing to convert discrete semantic anomaly events into continuous 0.2Hz GPS coordinate traces. Additionally, a comprehensive multi-layered noise model was implemented to emulate environmental signal degradation, including atmospheric drift and multi-path scattering, thereby narrowing the simulation-to-reality gap. In future work, we will focus on empirical benchmarking of the generated datasets against state-of-the-art trajectory anomaly detection algorithms to quantify their downstream utility.

#### References

- [1] [n. d.]. GitHub - valhalla/valhalla: Open Source Routing Engine for OpenStreetMap – github.com. <https://github.com/valhalla/valhalla/>.
- [2] Chanuka Algama, Taylor Anderson, Henrique Ferraz de Arruda, Andrew Crooks, Nathan Holt, Erfan Hosseini Sereshgi, John Hunter, Hamdi Kavak, Lance Kennedy, Yueyang Liu, Dieter Pfoser, Sandro Martinelli Reia, Doug Taylor, Mauryan Uppalapati, Boyu Wang, Carola Wenk, and Andreas Züfle. 2026. SF-LIFE: A Large-Scale Simulated Movement Dataset for the San Francisco Bay Area. arXiv:2606.00430 [physics.soc-ph] <https://arxiv.org/abs/2606.00430>
- [3] Hossein Amiri, Ruochen Kong, and Andreas Züfle. 2024. Urban Anomalies: A Simulated Human Mobility Dataset with Injected Anomalies. arXiv:2410.01844 [cs.SI] <https://arxiv.org/abs/2410.01844>
- [4] Liam Barkley and Brink van der Merwe. 2024. Investigating the role of prompting and external tools in hallucination rates of large language models. *arXiv preprint arXiv:2410.19385* (2024).
- [5] C3S. 2018. ERA5 hourly data on single levels from 1940 to present. doi:10.24381/CDS.ADBB2D47
- [6] Serina Chang, Emma Pierson, Pang Wei Koh, Jaline Gerardin, Beth Redbird, David Grusky, and Jure Leskovec. 2021. Mobility network models of COVID-19 explain inequities and inform reopening. *Nature* 589, 7840 (2021), 82–87.

- [7] Eunjoon Cho, Seth A. Myers, and Jure Leskovec. 2011. Friendship and mobility: user movement in location-based social networks. In *Proceedings of the 17th ACM SIGKDD International Conference on Knowledge Discovery and Data Mining* (San Diego, California, USA) (*KDD '11*). Association for Computing Machinery, New York, NY, USA, 1082–1090. doi:10.1145/2020408.2020579
- [8] Yuwei Du, Jie Feng, Jian Yuan, and Yong Li. 2025. CAMS: A CityGPT-Powered Agentic Framework for Urban Human Mobility Simulation. doi:10.48550/ARXIV.2506.13599 Version Number: 1.
- [9] Minxuan Duan, Yinlong Qian, Lingyi Zhao, Zihao Zhou, Zeeshan Rasheed, Rose Yu, and Khurram Shafique. 2024. Back to Bayesics: Uncovering Human Mobility Distributions and Anomalies with an Integrated Statistical and Neural Framework. In *Proceedings of the 1st ACM SIGSPATIAL International Workshop on Geospatial Anomaly Detection*. ACM, Atlanta GA USA, 56–67. doi:10.1145/3681765.3698454
- [10] Elisa Gallon, Mathieu Joerges, and Boris Pervan. 2021. Robust modeling of GNSS tropospheric delay dynamics. *IEEE Trans. Aerospace Electron. Systems* 57, 5 (2021), 2992–3003.
- [11] Song Gao, Jimeng Rao, Yuhao Kang, Yunlei Liang, and Jake Kruse. 2020. Mapping county-level mobility pattern changes in the United States in response to COVID-19. *SIGSPATIAL Special 12*, 1 (2020), 16–26.
- [12] Chengkai Han, Jingyuan Wang, Yongyao Wang, Xie Yu, Hao Lin, Chao Li, and Junjie Wu. 2025. Bridging traffic state and trajectory for dynamic road network and trajectory representation learning. In *Proceedings of the AAAI Conference on Artificial Intelligence*, Vol. 39, 11763–11771.
- [13] Thomas F Heston and Charya Khun. 2023. Prompt engineering in medical education. *International Medical Education* 2, 3 (2023), 198–205.
- [14] Erfan Hosseini Sereshgi, Mauryan Uppalapati, Yueyang Liu, Lance Kennedy, Andreas Züfle, and Carola Wenk. 2025. Semantic Anomaly Detection in Human Trajectories: Preserving Behavioral Patterns Through Calendar Representations. In *ACM SIGSPATIAL GeoAnomalies Workshop (GeoAnomalies '25)*. ACM, Minneapolis MN USA, 33–42. doi:10.1145/3764914.3770593
- [15] Xiaocheng Huang, Yifang Yin, Simon Lim, Guanfeng Wang, Bo Hu, Jagannadan Varadarajan, Shaolin Zheng, Ajay Bulusu, and Roger Zimmermann. 2019. GrabPosisi: An Extensive Real-Life GPS Trajectory Dataset in Southeast Asia. In *Proceedings of the 3rd ACM SIGSPATIAL International Workshop on Prediction of Human Mobility* (Chicago, IL, USA) (*PredictGIS'19*). Association for Computing Machinery, New York, NY, USA, 1–10. doi:10.1145/3356995.3364536
- [16] International GNSS Service (IGS). 1998. International GNSS Service (IGS) GNSS Final Daily Ionosphere Total Electron Content Grid product. doi:10.5067/GNSS/GNSS\_IGSIONOTEC\_001
- [17] Ziyi Jiang, Qiqi Wang, Xuyang Sun, Gillian Dobbie, Xiaoling Lu, Yalei Du, Yuanyuan Zhang, and Kaiqi Zhao. 2025. RECAST: Route-Enhanced Conditional Anomalous Sub-trajectory Detection. In *Proceedings of the 33rd ACM International Conference on Advances in Geographic Information Systems*. ACM, The Graduate Hotel Minneapolis Minneapolis MN USA, 357–369. doi:10.1145/3748636.3762745
- [18] Chenlu Ju, Jiaxin Liu, Shobhit Sinha, Hao Xue, and Flora Salim. 2025. Trajllm: A modular llm-enhanced agent-based framework for realistic human trajectory simulation. In *Companion Proceedings of the ACM on Web Conference 2025*. 2847–2850.
- [19] Joon-Seok Kim and Andreas Züfle. 2025. Grounded Anomalies: Towards Causally Grounded Kinematic Anomaly Generation. In *Proceedings of the 2nd ACM SIGSPATIAL International Workshop on Geospatial Anomaly Detection*. 1–10.
- [20] John A Klobuchar. 1987. Ionospheric time-delay algorithm for single-frequency GPS users. *IEEE Transactions on aerospace and electronic systems* 3 (1987), 325–331.
- [21] Ruochoen Kong, Hossein Amiri, Yueyang Liu, Lance Kennedy, Misha Gupta, Joon-Seok Kim, and Andreas Züfle. 2024. Human Mobility Challenge: Are Transformers Effective for Human Mobility Prediction?. In *ACM SIGSPATIAL HuMob Workshop*. 60–63.
- [22] Eva Krueger, Torben Schueler, and Bertram Arbesser-Rastburg. 2005. The standard tropospheric correction model for the European satellite navigation system Galileo. 23–29 pages.
- [23] Siyu Li, Toan Tran, Haowen Lin, John Krumm, Cyrus Shahabi, Lingyi Zhao, Khurram Shafique, and Li Xiong. 2025. Geo-Llama: Leveraging LLMs for Human Mobility Trajectory Generation with Constraints. In *2025 26th IEEE International Conference on Mobile Data Management (MDM)*. IEEE, 20–31.
- [24] Yihan Li, Xiyuan Fu, Ghanshyam Verma, Paul Buitelaar, and Mingming Liu. 2025. Mitigating Hallucination in Large Language Models (LLMs): An Application-Oriented Survey on RAG, Reasoning, and Agentic Systems. *arXiv preprint arXiv:2510.24476* (2025).
- [25] Ruirui Liu and Yiping Jiang. 2024. Overbounding multipath error in urban canyon with LSTM using multi-sensor features. *IEEE Transactions on Intelligent Transportation Systems* 25, 9 (2024), 10926–10940.
- [26] Yueyang Liu, Lance Kennedy, Hossein Amiri, and Andreas Züfle. 2024. Neural Collaborative Filtering to Detect Anomalies in Human Semantic Trajectories. In *Proceedings of the 1st ACM SIGSPATIAL International Workshop on Geospatial Anomaly Detection* (Atlanta, GA, USA) (*GeoAnomalies '24*). Association for Computing Machinery, New York, NY, USA, 79–89. doi:10.1145/3681765.3698463
- [27] Antonio Martellucci and Roberto Prieto Cerdeira. 2009. Review of tropospheric, ionospheric and multipath data and models for global navigation satellite systems. In *2009 3rd European Conference on Antennas and Propagation*. 3697–3702.
- [28] John Pesavento, Andy Chen, Rayan Yu, Joon-Seok Kim, Hamdi Kavak, Taylor Anderson, and Andreas Züfle. 2020. Data-driven mobility models for COVID-19 simulation. In *Proceedings of the 3rd ACM SIGSPATIAL International Workshop on Advances in Resilient and Intelligent Cities*. 29–38.
- [29] Claudio Picciarelli, Christian Micheloni, and Gian Luca Foresti. 2008. Trajectory-based anomalous event detection. *IEEE Transactions on Circuits and Systems for video Technology* 18, 11 (2008), 1544–1554.
- [30] Arun Sharma, Mingzhou Yang, Majid Farhadloo, Subhankar Ghosh, Bharat Jayaprakash, and Shashi Shekhar. 2025. Towards Physics-informed Diffusion for Anomaly Detection in Trajectories: A Summary of Results. In *Proceedings of the 2nd ACM SIGSPATIAL International Workshop on Geospatial Anomaly Detection*. ACM, Minneapolis MN USA, 11–24. doi:10.1145/3764914.3770595
- [31] Chris Stanford, Suman Adari, Xishun Liao, Yueshuai He, Qinhuo Jiang, Chenchen Kuai, Jiaqi Ma, Emmanuel Tung, Yinlong Qian, Lingyi Zhao, Zihao Zhou, Zeeshan Rasheed, and Khurram Shafique. 2024. NUMOSIM: A Synthetic Mobility Dataset with Anomaly Detection Benchmarks. arXiv:2409.03024 [cs.LG] <https://arxiv.org/abs/2409.03024>
- [32] Jiawei Wang, Renhe Jiang, Chuang Yang, Zengqing Wu, Makoto Onizuka, Ryosuke Shibasaki, Noboru Koshizuka, and Chuan Xiao. 2024. Large language models as urban residents: An llm agent framework for personal mobility generation. *Advances in Neural Information Processing Systems* 37 (2024), 124547–124574.
- [33] Shengyuan Wang, Jie Feng, Tianhui Liu, Dan Pei, and Yong Li. 2025. Mitigating Geospatial Knowledge Hallucination in Large Language Models: Benchmarking and Dynamic Factuality Aligning. In *Findings of the Association for Computational Linguistics: EMNLP 2025*. 870–888.
- [34] Haomin Wen, Shurui Cao, and Leman Akoglu. 2025. CoBAD: Modeling Collective Behaviors for Human Mobility Anomaly Detection. doi:10.48550/arXiv.2508.14088 arXiv:2508.14088 [cs].
- [35] Wilson Wongso, Hao Xue, and Flora D. Salim. 2026. Massive-STEPS: Massive Semantic Trajectories for Understanding POI Check-ins – Dataset and Benchmarks. arXiv:2505.11239 [cs.LG] <https://arxiv.org/abs/2505.11239>
- [36] Takahiro Yabe, Kota Tsoubouchi, Toru Shimizu, Yoshihide Sekimoto, Kaoru Sezaki, Esteban Moro, and Alex Pentland. 2024. YJMob100K: City-scale and longitudinal dataset of anonymized human mobility trajectories. *Scientific Data* 11, 1 (April 2024), 397. doi:10.1038/s41597-024-03237-9
- [37] Dingqi Yang, Daqing Zhang, Vincent W Zheng, and Zhiyong Yu. 2014. Modeling user activity preference by leveraging user spatial temporal characteristics in LBSNs. *IEEE Transactions on Systems, Man, and Cybernetics: Systems* 45, 1 (2014), 129–142.
- [38] Kunyi Zhang, Yanbo Pang, Yurong Zhang, and Yoshihide Sekimoto. 2024. MobGLM: A large language model for synthetic human mobility generation. In *Proceedings of the 32nd ACM International Conference on Advances in Geographic Information Systems*. 629–632.
- [39] Yu Zheng. 2011. T-Drive trajectory data sample.
- [40] Yu Zheng, Hao Fu, Xing Xie, Wei-Ying Ma, and Quannan Li. 2011. *Geolife GPS trajectory dataset - User Guide*.
- [41] Silin Zhou, Yao Chen, Shuo Shang, Lisi Chen, Bingsheng He, and Ryosuke Shibasaki. 2025. Blurred Encoding for Trajectory Representation Learning. *arXiv preprint arXiv:2511.13741* (2025).
- [42] Yuanshao Zhu, James Jianqiao Yu, Xiangyu Zhao, Xun Zhou, Liang Han, Xuetao Wei, and Yuxuan Liang. 2025. UniTraj: Learning a Universal Trajectory Foundation Model from Billion-Scale Worldwide Traces. *Advances in Neural Information Processing Systems* 38 (2025).